IMAGING INDUCED MICROSEISMICITY DURING THE 1993 INJECTION TESTS AT SOULTZ-SOUS-FORETS, FRANCE

[1]R H Jones, [1]A Beauce, [1]A Jupe, [2/3]H Fabriol and [1]B C Oyer

[1]CSM Associates Ltd, Rosemanowes, Herniss, Penryn, Cornwall, TR10 9DU, UK
[2]BRGM/IMRG BP 6009 45060 Orleans Cedex 2 France [3]Now at CICESE
Division Ciencias de la Tierra, Apdo. Postal 2732, Ensenada, B.C. Mexico

KEYWORDS

Microseismicity, fluid injections, HOR

ABSTRACT

As part of the 1993 work programme at the European Hot Dry Rock (HOR) site at Soultz-sous-Forêts a series of stepped injections with flow rates of up to 50 l/s were carried out over an openhole section from 2850 to 3600 m measured depth in the borehole GPK1. In total around 45,000 m^3 of water were injected during September and October 1993.

During the injection tests about 19,000 micro-earthquakes were recorded of which some 16,000 have been located. The typical event rate was over one thousand a day and seismic monitoring was continuous throughout the experimental period. The imaged seismic cloud is seen to contain several distinct features with azimuths varying from N-S to NW-SE. A strong correlation between flow and seismicity is also observed.

1 INTRODUCTION

Experiments have been conducted since 1987 at the European Hot Dry Rock research site at Soultz-sous-Forêts, Alsace, France (Baria et al., 1992). In Phases I (1987-88) and IIa (1991) investigations were made into the hydraulic behaviour of the granite at depths of around 2000 m using the borehole GPK1. During Phase IIa two 50 hour injection tests with injection rate of 7 l/s and 15 l/s were performed and a network of three-component seismic sensors were used to detect and locate 370 micro-earthquakes (Beauce et al., 1992). These micro-earthquakes formed a NW-SE elongated cloud in the depth range 1800 to 2250 m.

In 1992 the borehole GPK1 was extend from 2000 m to 3600 m depth, reaching a bottom hole temperature of 160°C. The purpose of the 1993 experimental programme was to characterise the hydraulic behaviour of the granite rockmass over the openhole section of the GPK1. This paper describes the results of the microseismic monitoring of these injection tests.

2 THE SEISMIC MONITORING SYSTEM

Experience in HOR microseismic monitoring has shown that in order to maximise the number of micro-earthquakes detected it is necessary to place the seismic sensors in the crystalline basement within which the seismic activity takes place, and below any attenuating sedimentary cover which may be present (Jones 1989). In the case of Soultz this required the seismic sensors to be placed in sondes deployed in old recovered oil wells.

For the experiments described here three such oil wells were used and the sondes were deployed at depths between 1400 and 1600 m. The temperature in these seismic observations wells it these depths is about 125°C. The seismic sondes were designed to operate at temperatures of up to 150°C and to operate for at least five years.

Thus the permanent seismic network consists of only three observation boreholes. Accelerometers were used as the sensors in the seismic sondes. In order to increase the quality and reliability of the data acquired from each sonde and to increase the redundancy of the network a novel sensor configuration was adopted for these sondes.

The standard sensor configuration for a multi-component seismic sonde is to mount three sensors orthogonally. The obvious disadvantage with the three component orthogonal configuration is that it possesses no inherent redundancy. If any one of the three sensors fails then the three-dimensional nature of the data is lost. Indeed a more subtle problem with the orthogonal three component configuration is that if the sensitivity or gain of one of the sensors varies this cannot be diagnosed from the data recorded.

As the seismic sondes were to be deployed permanently, with an expected lifetime of five years and at temperatures of around 125°C it was decided that some degree of redundancy would be desirable. In order to achieve this a four component equi-angular configuration was adopted. The four sensors can be thought of as being arranged such that they each lie on one of the four vectors pointing out from the centre of an equilateral Tetrahedron. In the actual sonde the sensors are arranged in a vertical column but with the appropriate angles between sensors preserved.

Matrix analysis of this configuration shows it to be optimum configuration for four sensors and further shows that if any one of the sensors fails the performance of the remaining three sensors is 82% of that of the performance of a traditional three component configuration (Jones 1992).

Two of the three sondes were cemented in place at the bottoms of their respective boreholes and the third was deployed in viscous mud at the bottom of the third borehole. The sondes are deployed on standard seven-core logging cable which is used to supply power to the sonde and carry the signal to the surface.

The sub-surface network is completed by either a single or a pair of hydrophones deployed in an observation borehole, EPS1, at depth of 2100 m and a temperature of 145°C. The hydrophones are deployed just for the period covering the hydraulic injections and removed after the seismic activity associated with the injections has ceased.

The signals from the seismic network are cabled back to a central data acquisition centre where they are anti-alias filtered before being digitised at a rate of 5000 samples per second per channel. The data acquisition system is based on two Sun workstations, one controls the various processes and file handling while other continuously examines the incoming digitised data for micro-earthquake signals.

Conceptually the system is based on a software ring buffer configuration. The digitised data are split, one version is passed to memory which is configured as a ring buffer and the other copy is passed to the software trigger. If a seismic signal is detected by the software trigger then the appropriate portions of the data are extracted from the ring buffer memory and written to disk for further analysis. The system is configured such that overlapping portions of data can be written to disk from the ring buffer. This ensures that there is no 'down time' between micro-earthquake detections. This is important as micro-earthquakes often occur in swarms.

The data acquisition system runs under **UNIX** and is multi-tasking thus captured micro-earthquakes can be plotted, analysed and located while the system is continuously running without degrading the system performance. Any locations produced can also be displayed and plotted onto hardcopy during acquisition. This is important especially during injection experiments which may last several weeks when decisions about the future course of the experiment depend critically on the information provided by the imaged seismicity.

The seismic velocity structure was determined prior to the start of the injections by firing a series of calibration shots in the borehole **GPK1.** An isotropic velocity structure was adopted with station delays of a few milliseconds for the various stations.

3 THE 1993 HYDRAULIC INJECTION PROGRAMME

The hydraulic injection programme consisted of five main tests (Jung 1994). The first test was a production test and the second test consisted of a series of injections below a packer set at 3560 m. However the packer soon failed and then the borehole was sanded up to a depth of 3400 m. Microseismic activity close to the packer was observed during the injection.

The third test, which is referred to here as the September openhole test, was a large scale injection using steps up to 36 l/s in which a total volume of 25,000 m^3 of water was injected. The borehole was open from the casing shoe, 2850 m, to a depth of 3400 m for this test and it was during this period that the majority of the seismicity occurred, around 17,000 events. The well was then shut in for three days.

The fourth test was designed to stimulate a hydraulically significant feature encountered at 3485 m depth. The sand was washed out to a depth of 3507 m and a double packer set at 3457 m. After 440 m^3 of water had been injected a hydraulic connection was detected across the double packer and the test was stopped. Around 100 microseismic events clustered around the short openhole section were observed during the injection.

For the fifth and final test, which is referred to here as the October openhole test, the remaining sand was washed out and the packers removed. A total of 19,300 m^3 of water was injected over the total openhole section at rates of 40 l/s (for 4 days) and finally 50 l/s (for one day). Around 1700 microseismic events were detected during this test.

4 RESULTS OF THE MICROSEISMIC MONITORING

A total of around 19,000 microseismic events were detected of which almost 16,000 have been located. All microseismic events were examined, timed and located manually rather than automatically. This was required because of the sparse nature of the network and to ensure the accuracy of the locations.

The waveforms from a four component sonde for a typical micro-earthquake are shown in Figure 1. The p-wave is most clearly visible on the vertical component and the onset of the s-wave can be seen on the three sub-horizontal components. This type of waveform indicates that shearing along pre-existing joints is the main mechanism of seismic energy release (Fehler 1989) Typical signals contain significant energy up to frequencies of several hundred Hz are routinely observed and the grouting and design of the four-component sondes ensures that they are free of resonances in this frequency band. Timing accuracy is of the order of a millisecond to a few milliseconds and the relative location accuracy is modelled as being typically as of the order of a few tens of metres. This is confirmed by the scale of the distinct features imaged in the seismic results presented below.

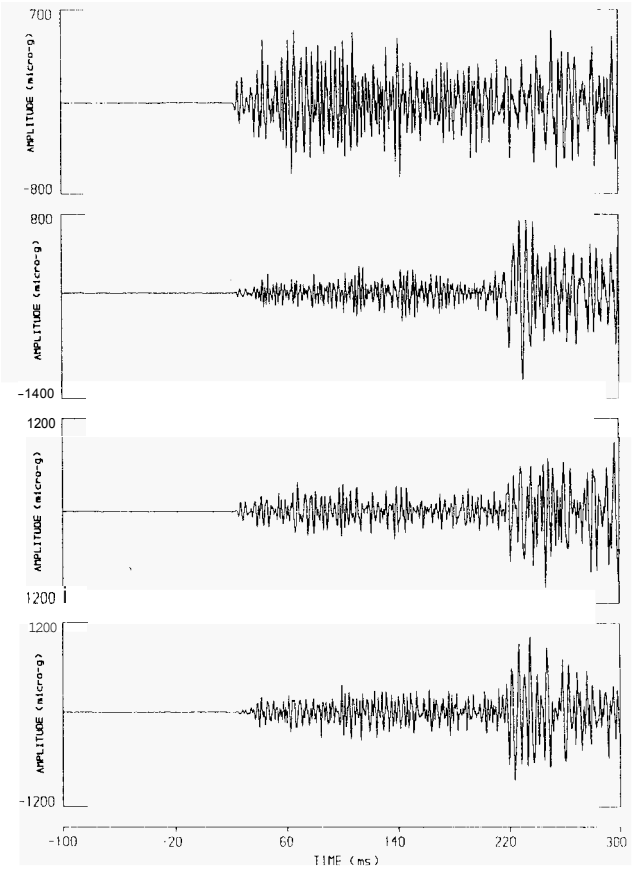

Figure 1 Time histories for a typical micro-earthquake recorded on a four-component sonde. The top trace is the vertical component, the other three being sub-horizontal.

After presenting maps of the seismicity produced several specific aspects of the data are examined in more detail, specifically; the seismicity from the September and October openhole tests, the correlation between seismicity and flow and the strike of the seismic cloud versus depth.

Figure 2 shows three orthogonal views of all the located seismicity. The plan view shows that the main direction of horizontal growth is **NW-SE** but other distinct growth directions are seen within the overall cloud.

The view from the South-West shows that the most intense region of seismicity is centred on the borehole at a depth of 2900 m and shows that there is an overall tendency for the microseismic cloud to grow upwards as well as horizontally. Again as in the plan view of the seismicity distinct regions of seismicity can be distinguished.

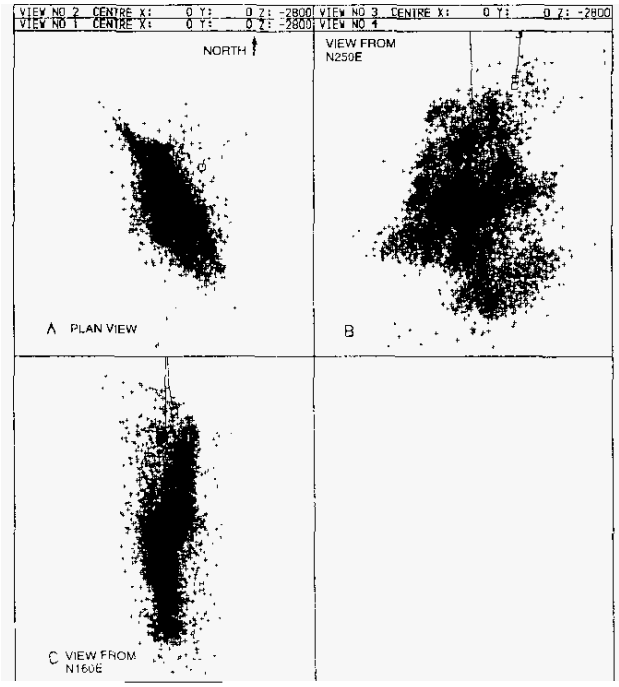

Figure 2 Three orthogonal views of the microseismic cloud. Plan view (A), and two side elevations from N250E (B) and N160E (C).

4.1 The September openhole seismicity

Although this was the third test in the programme it was the first openhole injection test (2850 - 3400 m). A summary of the injection flow rate, surface injection pressure and depth of located seismicity is given in Figure 3. The initial injection rate was 0.15 l/s and this was increased in a stepwise manner as shown in Figure 3. Microseismic activity started at an injection flow Pate of 6 l/s and a surface injection pressure of around 6 MPa (60 bar).

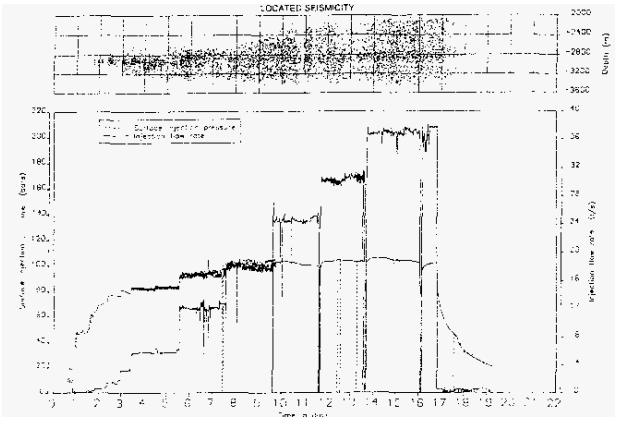

Figure 3 Synapsis of the September injection tests showing the surface injection rates. pressures and seismic activity.

The initial seismicity was all located within 100 m of the borehole and near the casing shoe in the depth range 2800 to 3000 m. As the injection proceeded the rate of seismicity substantially increased with the surface injection pressure at around 8 MPa (80 bars). The seismicity at this point is approximately radially distributed around the borehole and grows downwards to cover the entire openhole section of the borehole.

Once the depth extent of the seismicity is approximately the same as that of the openhole section the seismicity then shows a tendency to grow upwards. This occurs after the injection rate is increased to 18 *l/s* and the surface injection pressure stabilises at 10 MPa (100 bar), A distinct elongation of the seismic cloud in a NW-SE direction is seen, with the majority of the activity being to the northern side of the openhole. The seismicity continues to show upwards growth with some locations being as shallow at 2000 m, but very few locations are found much below the bottom of the openhole. Several N-S striking features can be seen within the cloud. and these are considered further in a subsequent section.

4.2 The October openhole seismicity

In this injection test the openhole hole now extends from 2850 to 3600 m. The openhole section from 2850 to 3400 m having previously been exposed during the September openhole experiment. Around 90% of the flow left the borehole in the previously exposed section of the well.

For the first 3.5 days of the injection at 41 l/s the seismicity is almost entirely confined to the vicinity of the newly exposed section of well, only after about 12,000m^3 of water had been injected did significant seismic activity occur in the previously seismically active upper zones. The evolution of the seismicity over this period and in comparison with the September openhole data is shown in Figure 4. The observed behaviour indicates that the' previously stimulated upper zones must be re-pressurized and re-inflated before further shearing can occur.

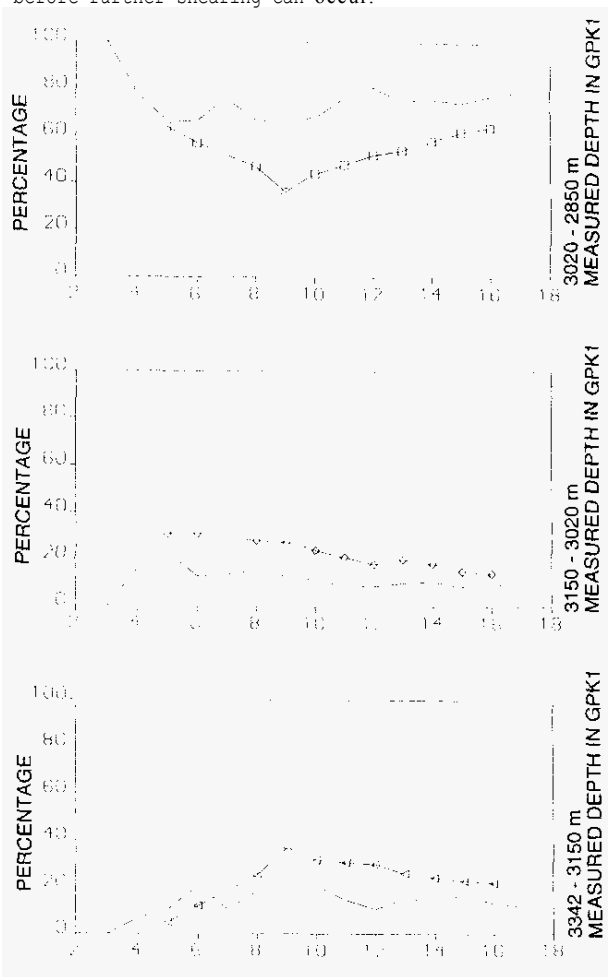

Figure 4 Proportions of flow exit (line with symbol) and seismic activity (plain line) for the three flowing zones varying with time for the September injection tests.

4.3 The correlation between flow and seismicity

Flow logs were run on a daily basis during the September injection tests (2850 - 3400 m). These logs showed that the well could be reasonably divided into three distinct flowing zones. The upper zone. which took most of the flow (2850 - 3020 m), the middle zone (3020 - 3150 m) which took progressively less flow as the injections proceeded and the lowest zone (3150 - 3342 m) which initially took only 5% of the flow although this increased to a peak of around 37% on September 9 before decreasing back to 20%.

To examine the relationship between flow and seismicity the depths of the located seismicity determined for the September injection tests have been divided up into the same zones as those of the flow logs. The two sets of data are plotted for comparison in Figure 5 where both flow and seismic activity are displayed as percentages.

The relationship between fluid flow and microseismicity plays a crucial role in determining the usefulness of microseismic mapping as a technique in analysing HOR reservoirs (CSMA, 1992). The correlation shown in Figure 5 and the behaviour discussed in the previous section suggest that, at least for the current site, there is a strong correlation between flow and seismicity when (1) good quality data is available and (2) the rockmass is previously unstimulated.

4.4 The orientation of the seismic cloud versus depth

In the plan view in Figure 3 several distinct features with differing azimuths can be seen. Figure 6 shows the same location data as the Figure 3 plan view but the data are now divided into depth slices, the position of the openhole within the seismic cloud is indicated by a white square.

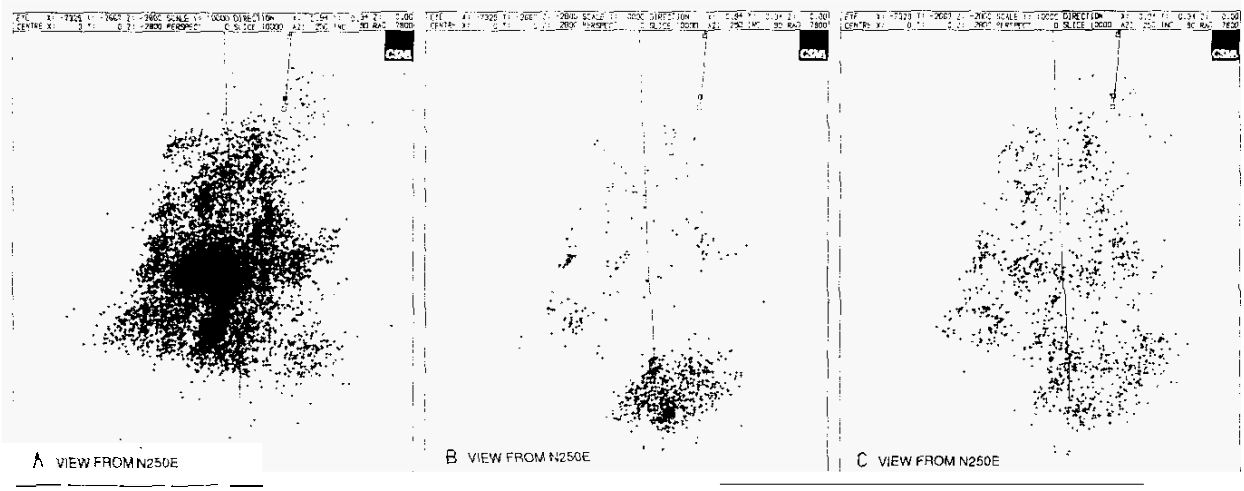

Figure 5 Time evolution of the seismic cloud. The September seismicity (A) compared with the early (B) and late (C) October seismicity. All elevations are from N250E (as in Figure 38)

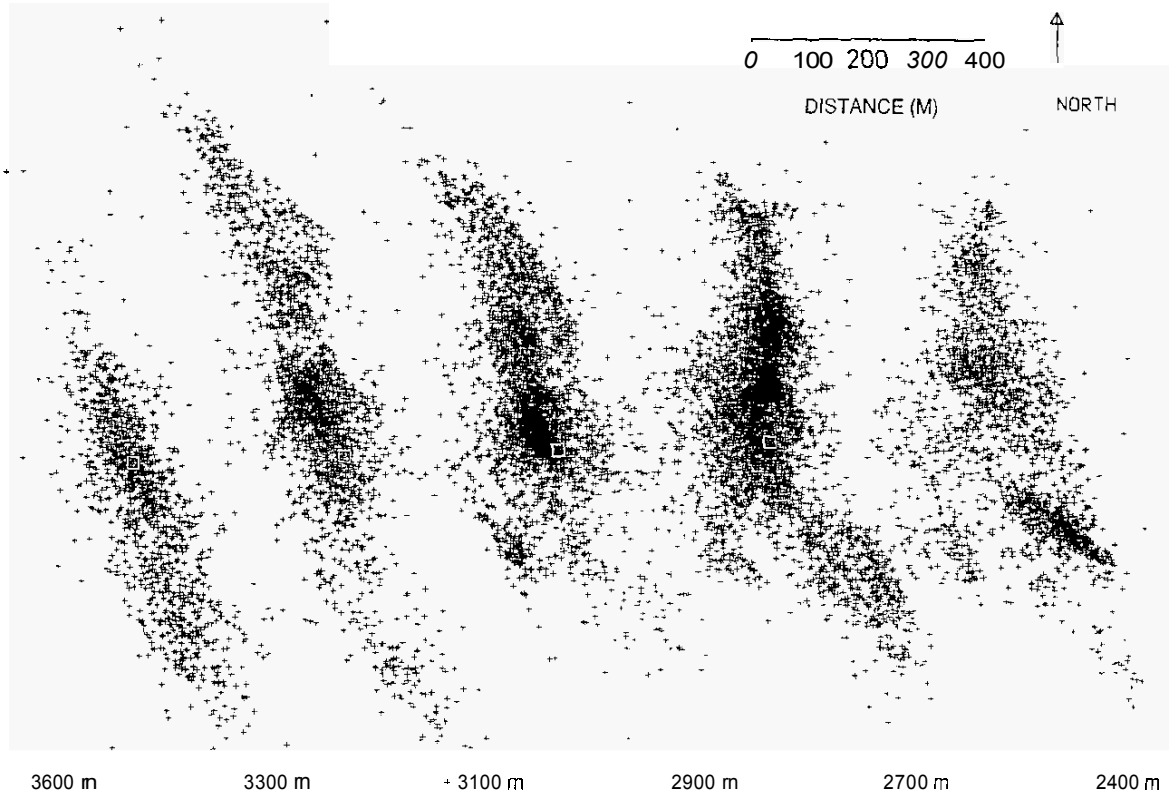

Figure 6 Depth slices through the seismic data showing the azimuth varying with depth. The openhole is indicated by a white square.

The dominant trends within the data range from NW-SE to N-S. A strong shallow feature with a NW-SE strike can be seen in the southern section of the cloud. In the depth range 2700 to 2900 m, the region where most of the flow exited the borehole the cloud takes on a distinct appearance. To the north of the borehole, where the seismic activity is most intense, the cloud strikes almost N-S and to the South of the borehole, where the seismicity is less intense. the cloud has a more **NW-SE** trend. Below this depth the cloud is defined by an overall trend of NNW-SSE but still with some smaller scale features striking with different azimuths.

In the area of interest the vertical stress *is* believed to just exceed the principle horizontal stress which is thought to strike at about N170E (Garnish et al.. **1994).** This azimuth is aligned with that of the intense region of seismicity to the northern side of the borehole around 2800 m depth. However the majority of the seismic cloud has a different strike, even at the 2800 m depth for the section of the cloud to the south of the GPK1 the strike is not N-S but NW-SE.

This would suggest that the pattern of jointing to the south and north of the well in this depth region are not the same. The presence of several distinct strike directions for different sections of the seismic cloud suggest variations in the jointing patterns within the rock in the region of the seismicity.

5 CONCLUSIONS

Mapping of the microseismic activity induced during major injections in GPK1 has produced images of seismicity containing distinct features with a range of azimuths within the overall cloud. The seismic cloud cannot be considered to be formed of a uniform volume of stimulated rock.

A strong correlation between seismicity and flow has been observed for injections into undisturbed rock at the Soultz site, and it has been seen that this correlation breaks down for repeated injections into the same openhole section of well.

At the time of writing the exact nature of the interaction between the jointing, in situ stresses and fluid flow within the **rock** cannot be considered to have been completely resolved.

The next step for the development of the European HDR site at Soultz is the drilling of a second well, GPK2, to establish a circulation loop. One of the main criteria for targeting this well is the microseismicity. Thus the further study and greater understanding of the microseismic data, and the role it **plays** in elucidating the interaction between the jointing. in situ stress and fluid pressure and flow, is of central importance to future success.

REFERENCES

Baria R., Baumgartner J., Gerard A., and Kappelmeyer O. (1992). HDR project at Soultz-sous-Forêts. Geothermal Resources Council Transactions, 16, 387-394.

Beauce A.. Jones R H., Fabriol H., Twose C., and Hulot C. (1992). Microseismic Monitoring of hydraulic experiments undertaken during phase IIa of the Soultr HDR project (Alsace. France). Proceedings. 17th ***Workshop on*** *Geothermal* Reservoir *Engineering*, Stanford University, Stanford, California, January 29-31, SGP-TR-141, 253-258.

CSM Associates Ltd 1992. Review of *HDR measurement* techniques. **CSM** report **No** IR02/08 prepared for AEA Technology Contract E/5A/164/2873.

Fabriol H., Beauce A., Genter A., and Jones R H. (1994). Induced Microseismicity and its relation with natural fractures: The HDR example of Soultz (France). Paper presented at the Annual Meeting of the Geothermal Resources Council. Salt Lake City, Utah, 2-5 October 1994.

Fehler M C, 1989, Stress control of seismicity patterns observed during hydraulic fracturing experiments at the Fenton Hill Hot Dry Rock Geothermal Energy Site, New Mexico, International *Journal* of Rock Mechanics and Mining Sciences and Geochemical Abstracts, vol 76, no 3/4, p211-219

Garnish J., Baria R., Baumgartner J. and Gerard A. (1994). The European Hot Dry Rock Programme 1994-95. Paper presented at the Annual Meeting of the Geothermal Resources Council, Salt Lake City, Utah, 2-5 October 1994.

Jones R. (1989). Analysis of microseismic ***data*** from the Soultz site, CSMA internal technical note TN03/45.

Jones R. (1992). Analysis of multi-component seismic sondes, CSMA internal technical note TN03/102.

Jung R. **(1994).** Hydraulic tests *Summer/Autumn 1994*, BGR field report.